Heliyon 10 (2024) e27007

Contents lists available at ScienceDirect

Heliyon

journal homepage: www.cell.com/heliyon

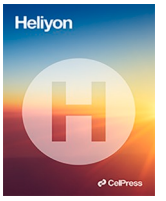

Research article

Modeling benefits and tradeoffs of green infrastructure: Evaluating and extending parsimonious models for neighborhood stormwater planning

Moira L. Zellner *, Dean Massey

School of Public Policy and Urban Affairs, College of Social Sciences and Humanities, Northeastern University. 310 Renaissance Park, 1135 Tremont St, Boston, MA 02115, USA

ARTICLE INFO

Keywords:
Stormwater management
Hydrologic modeling
Stormwater pollution
Green infrastructure planning
Agent-based modeling
Green infrastructure benefits and tradeoffs

ABSTRACT

Green infrastructure is often proposed to complement conventional urban stormwater management systems that are stressed by extreme storms and expanding impervious surfaces. Established hydrological and hydraulic models inform stormwater engineering but are time- and data-intensive or aspatial, rendering them inadequate for rapid exploration of solutions. Simple spreadsheet models support quick site plan assessments but cannot adequately represent spatial interactions beyond a site. The present study builds on the Landscape Green Infrastructure Design (L-GrID) Model, a process-based spatial model that enables rapid development and exploration of green infrastructure scenarios to mitigate neighborhood flooding. We first explored how well L-GrID could replicate flooding reports in a neighborhood in Chicago, Illinois, USA, to evaluate its potential for green infrastructure planning. Although not meant for prediction, L-GrID was able to replicate the flooding reported and helped identify strategies for flood control. Once evaluated for this neighborhood, we extended the model to include water quality through the representation of dispersion and settling mechanisms for two pollutant surrogates—total nitrogen and total suspended solids. With the extended model, Landscape Green Infrastructure Design Model-Water Quality (L-GrID-WQ), we examined benefits, costs, and tradeoffs for different green infrastructure strategies. Bioswales were slightly more effective than other green infrastructure types in reducing flooding extent and downstream runoff and pollution, through increased infiltration and settling capacity. Permeable pavers followed in effectiveness and are suggested where spatial constraints may limit the installation of bioswales. Although green infrastructure supports both flooding and pollution control, small tradeoffs between these functions emerged across spatial layouts: strategies based on only curb-cuts better controlled pollution, while layouts that followed the path of water flow better controlled flooding. By illuminating such tradeoffs, L-GrID-WQ can support green infrastructure planning that prioritizes unique concerns in different areas of a landscape.

1. Introduction

Climate change is shifting annual precipitation totals and increasing its variability [1]. Although some areas are forecasted to

* Corresponding author.
E-mail addresses: m.zellner@northeastern.edu (M.L. Zellner), de.massey@northeastern.edu (D. Massey).

https://doi.org/10.1016/j.heliyon.2024.e27007
Received 1 December 2023; Received in revised form 19 February 2024; Accepted 22 February 2024
Available online 5 March 2024

become wetter in the coming decades [2,3], even areas predicted to be dryer will experience greater frequency of extreme storms. The resulting increased urban runoff will wash more pollutants into treatment plants and water bodies [4]. Treating pollutants in runoff with conventional graywater systems is already costly for governments and ratepayers [5,6] and additional climate-change induced runoff will increase this burden [7–11]. Growing urbanization will only compound the problem [1,6,12]. Climate change also increases the uncertainty in both weather forecasts and appropriate stormwater management approaches [13]. The lack of flexibility of conventional gray infrastructure systems makes them ill-suited to handle the uncertainty of climate change [6,14–16]. Furthermore, increasing local sewer capacity—wherever there may be resources to do so—merely shifts the problem downstream, where sewer outlets ultimately discharge [17]. Conventional systems are also optimized for removing nutrients and organic matter but not the remaining harmful matter, including heavy metals, fine particles, and pesticides [18,19] that are then discharged with treated water.

Use of green infrastructure (GI) for stormwater management of water quantity and quality is increasingly common [20–22] as a way to increase stormwater system flexibility and reduce its maintenance costs and carbon footprint [23]. GI seeks to divert water from conventional stormwater systems to devices designed to mimic natural processes to detain, retain, infiltrate, or filter water away from where it can cause harm [24]. Examples of these devices are green roofs, rain barrels, bioswales/bioretention devices, and permeable pavers. Studies and reviews have shown the effectiveness of GI in alleviating flooding and improving water quality, with some variability in performance [22,24–29]. While GI can still be expensive, it presents opportunities to flexibly enhance urban environments and respond to a range of local and regional problems that are exacerbated by climate change, such as heat island effects, loss of wildlife habitats, air pollution, and poor public health [24,27,30–32,32–35]. The flexibility and cost-effectiveness of GI are especially critical for municipalities that lack the funding for large gray infrastructure projects.

Despite its benefits, GI alone cannot eliminate all urban flooding [22,27,36,37]. Sewers will remain essential in large storms [38], especially where there is little space for GI. Due to its flexibility, GI can supplement gray infrastructure [14,34,39–41], but only up to a certain extent. Both GI and gray infrastructure can quickly be overwhelmed by larger storms unless GI coverage is significantly expanded. Nevertheless, GI can effectively alleviate flooding in smaller storms, even at lower coverage values, when accounting for the spatial configuration of the infrastructure [37].

Addressing questions about the amount and spatial layout of GI coverage needed to alleviate neighborhood flooding and associated pollutant loads requires exploratory modeling to easily test how GI fits within the broader urban landscape, and the features that contribute to the quantity and quality of flooding, e.g., impervious cover (pollutant wash-off and runoff generation), sewer conditions (removals from the landscape), and elevation (where surface water flows). The ability to conduct such explorations is particularly important for pollution because water quality effects take time and resources to be identified and assessed through specialized analysis [24]. Exploratory approaches to modeling can also help understand tradeoffs between different GI scenarios (e.g., costs, damages, infiltration and recharge, socio-environmental co-benefits), which tend to be neglected in the literature [17,35,42,43]. Established models tend to be computationally expensive and require modeling expertise and calibration data that make this kind of exploration difficult and expensive, especially for local communities. The availability of user-friendly and nimble process-based models that capture the relevant hydraulic/hydrological and pollution transport mechanisms to inform green infrastructure planning is critical for such communities to be able to envision, assess and reap the multiple benefits of these kinds of interventions.

In this paper, we explain the need for exploratory modeling to support the rapid design and testing of GI scenarios and present an evaluation and extension of a model to cover this need. The Landscape Green Infrastructure Design (L-GrID) model [37] is a high-resolution, spatially explicit, process-based model that allows for the rapid development and exploration of GI placement scenarios. The model is publicly available,[1] and can be adapted to a variety of different landscape, environmental, and storm conditions. Its availability, flexibility, ease of parameterization, and computational speed makes it well-suited to inform local GI planning. While the model reportedly generated stormwater management recommendations in line with expert knowledge (John Watson, Metropolitan Water Reclamation District of Greater Chicago (MWRD), pers. comm., 2019; James Yurik, MWRD, pers., comm. 2018) and other studies [44], we attempt here to evaluate its ability to replicate observational flooding data in an area of Chicago, Illinois, USA, and extend it to represent water quality to assess the flooding and pollution control benefits and tradeoffs provided by a range of GI types and layouts in the same area. Finally, we derive implications for both modeling and policy.

2. Theory and calculation

2.1. Stormwater management and modeling needs

Existing flooding models can range from simple spreadsheet tools designed to estimate impacts of development—such as the US Department of Agriculture's Urban Hydrology for Small Watersheds (TR-55) [45] and Purdue University's L-THIA [46]—to stand-alone, data-intensive programs to design management practices—such as SUSTAIN [47] and perhaps the most commonly used software, SWMM [48]. Similar but proprietary models include MUSIC (and the newer MUSICX) [49] and MOUSE (now in the MIKE software suite) (e.g. Ref. [50]).

Tools like TR-55 and L-THIA are intended for single site assessment and are not spatially or temporally explicit, but they can be adapted to gain general insights at larger scales. Xu et al. [51] used L-THIA and SUSTAIN to develop what they call the Marginal-Cost-based Greedy Strategy, a computationally-intensive optimization algorithm to guide placement of GI. The general

[1] The code can be requested here: https://cssh.northeastern.edu/policyschool/participatory-modeling/.

recommendations align with prior studies with more parsimonious models [37,52], whereby GI should be placed where it can be readily reached by runoff and where monetary investment and achievement of environmental goals are maximized, while large investment levels return diminishing environmental benefits. Chen et al. [53] extended L-THIA to evaluate the lifetime costs and benefits of GI scenarios, where combinations of GI types performed better than single types, but more GI did not always translate into better results and best performing scenarios required impractically large amounts of GI.

Spatially and temporally explicit models like SWMM and SUSTAIN are data intensive, may need substantial calibration, and require great amounts of time and technical expertise to operate. However, they have built in optimization tools [33] that can be used to explore GI allocation. For example, Mei et al. [22] found that in isolation, vegetated swales provided by far the most benefits compared to bioretention cells, permeable pavement, and green roofs, but that using bioretention cells and vegetated swales together provided the most cost-effective outcome. None of the scenarios tested were capable of eliminating flooding, however, consistent with findings from Moore et al. [36], and other studies using simpler models (see above). Chen et al. [54] found that relative performance of GI scenarios varied greatly across sites, but their subsequent quantitative validation revealed that SUSTAIN's processes were highly sensitive to infiltration rates—thus explaining the highly variable scenario outcomes—prompting the need for empirical calibration for each area modeled.

The data resources and computational complexity required to use these models and make sense of the results do not allow the rapid exploration of a wide range of scenarios to support GI planning, particularly at the municipal or neighborhood level. Data-intensive modeling discourages stakeholder involvement, remaining mostly as academic studies or regulator-sponsored research. Participatory processes can allow people to better understand how GI works and open dialogues about what solutions are better for everyone [42]. Even when engaging stakeholders in GI modeling (e.g. Refs. [55,56]), the complexity of the models gets in the way of progress towards implementable solutions. Simulation speeds matter to inform deliberations in real time. High-resolution representation of neighborhoods can show the explicit distribution of impacts and tradeoffs, revealing deeper insights into strategies that work, such as why clustering of GI might be more effective for steep slopes [43], but much less effective in flat landscapes [37]. Additionally, although optimization programs and algorithms exist—see Zhang & Chui [33] for an exhaustive review of spatial allocation optimization tools (SAOTs)—purely algorithmic site selection prevents stakeholders from engaging in understanding flooding through modeling, in a way that can inform the deliberation of tradeoffs to support democratic decision making.

2.2. The L-GrID model and its water quality extension

In its original version, the L-GrID model is a cellular model created in NetLogo [57], with a single, stylized form of GI that incorporated features common to various types, mainly the capacity of a generalized bioswale to infiltrate and store stormwater [37]. For the work presented here, L-GrID was extended to include new GI types and to represent water pollution processes; hereon we refer to the updated model as L-GrID-WQ. The model allows users to modify storm duration, landscape size, GI placement, sewer configuration, and coverage ratios for different land cover types. After the configuration is set, the user can run simulations and compare results across several different metrics of water quality and quantity, as well as costs associated to the investment and damages. The easy comparison of outputs and tradeoffs across GI scenarios allows users to examine the effectiveness of each relative to each other and to a baseline without GI, while also deriving generalized principles for GI planning. L-GrID and L-GrID-WQ are not intended as forecasting or engineering tools; other modeling tools described above (e.g., SWMM) are better suited for that purpose. Nonetheless, groups with both high and low technical expertise have successfully used L-GrID and endorsed its findings for GI planning (John Watson, MWRD, pers. comm., 2019 [52]).

Below we detail the landscape elements of the L-GrID-WQ model and the algorithms representing the various dynamic processes in the order in which they are executed in the model, focusing on the water quality extension. We follow this model description with parameterization and sensitivity testing, an evaluation of the model's ability to replicate observed flooding, a description of the new output metrics to account for pollution effects, and the description of the GI scenarios to be tested with the extended model.

2.2.1. Landscape elements

The landscape elements of L-GrID-WQ expand on the first released version of L-GrID (Fig. 1) to include diverse and customizable

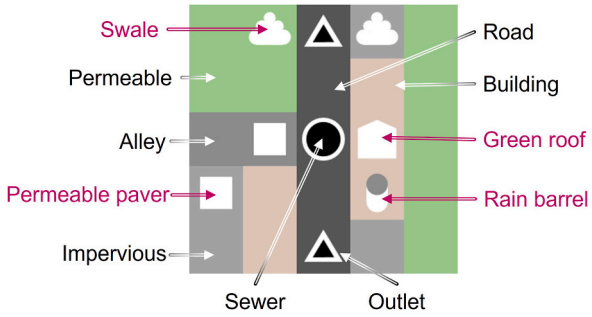

Fig. 1. New L-GrID-WQ landscape elements (in magenta) are customizable GI types, placed in permitted areas.

types of GI. To avoid duplication with Zellner et al. [37], we focus here on the extensions introduced to the model. Default parameters correspond to an area in Chicago, Illinois, USA, and are listed in the Appendix, along with references for model assumptions.

The landscape is a two-dimensional lattice of cells. The resolution can be set by the user; for all simulations in this study, cells are 10 m $\times$ 10 m. This resolution is set to match the width of a US city street, since streets are the main channels for stormwater flow in urban environments. While the original version of L-GRID could only load a generic, stylized landscape using sliders that determine its size and land cover, L-GrID-WQ allows users to import a landscape using input files corresponding to a real landscape. All input files must represent a rectangular landscape, but the area modeled may be irregularly sized; cells that must be excluded from computation are identified with a dummy land cover value.

2.2.1.1. Sewers. Sewer inlets are placed along streets at regular, user-defined intervals. Alternatively, users can import a landscape where cells may have more than one inlet (e.g., when inlets are clustered at intersections), in which case they will share the drainage into the sewer system. Inlets have a base intake rate, which can be adjusted with an input file to reflect different conditions.

2.2.1.2. Green infrastructure types. L-GrID was extended to include three more GI types in addition to the original bioswales: rain barrels, green roofs, and permeable pavers. Performance parameters and installation and maintenance costs can be adjusted in the code.

As in the original L-GrID, bioswales in L-GrID-WQ can be placed on permeable or impervious cover. The soil is engineered to

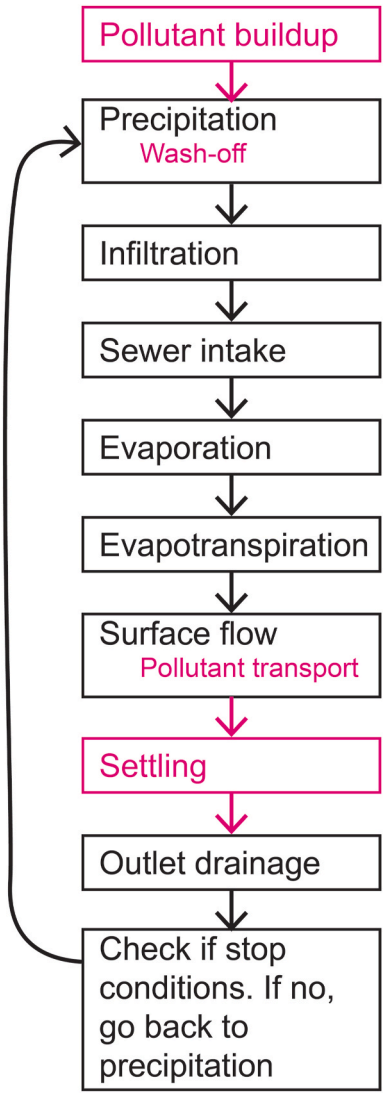

Fig. 2. Order of events highlighting the new (sub)processes (in pink). (For interpretation of the references to colour in this figure legend, the reader is referred to the Web version of this article.)

enhance infiltration, and surface storage is added to further collect ponded water. If they are next to roads, their elevation is lowered to represent curb-cuts, which allows water to flow directly from the street into the bioswale. Rain barrels are assumed to have a small, fixed volume of storage and can only be placed on buildings to represent their connection to building rain gutters. All water that falls on a building having a rain barrel will go directly into the barrel's storage until its capacity is reached, and any additional precipitation becomes runoff. Green roofs can be placed only on buildings and retain a volume of water that is relative to the depth and composition of engineered soil; any excess becomes runoff. Permeable pavers can be placed on impervious cover that is not a building or a road. This GI type represents a depth of engineered soil that infiltrates precipitation and drains into the sewer system, so pavers will both retain and detain water. Infiltration rates and storage volumes of all GI types are determined by soil properties (see Appendix) and by Virginia's BMP Design Specifications [58].

Total costs reflect the present value for the installation year plus 20 additional years of maintenance, the assumed infrastructure life cycle (see Appendix). Monetary costs are based on per unit area estimates taken from recent literature. These costs are adjusted for inflation [59] and geographic region [60], and are calculated assuming a 7% discount rate [61] and projected inflation rates [62]. Project costs only account for the GI itself, not the larger set of improvements that typically surround GI installation, such as street and sidewalk repairs, grading changes, landscape beautification, or new lighting and street furniture.

GI elements are placed by the user to create GI scenarios. GI may be partially full before the start of a storm event, to simulate the effect of frequent events (see hydrological scenario in the Appendix). The capacity already in use in this manner is set by sliders.

2.2.2. Processes and order of execution

The order of processes executed in the model builds on the first released version of L-GrID. To avoid duplication with Zellner et al. [37], we summarize the main water transport algorithms and focus on detailing the extensions to the model (Fig. 2). The default parameter values for all model processes are listed in the Appendix. The default time step for simulations is 1 min.

The original version of L-GrID includes the following processes: precipitation, infiltration, sewer intake and treatment, evapotranspiration, surface flow, and watershed export to downstream areas. The algorithms modeled for these processes were derived from established hydrologic models and local Chicago data, together with expert knowledge from local water managers and engineers. Users can modify rainfall duration that the model adapts as a hyetograph to vary rainfall over the duration of a storm, landscape size, placement of GI, sewer configuration, and the percentage of different land cover types. After configuration, simulations can be run and compared across flooding metrics: flooded area, and volume of runoff conveyed to sewers, GI, and adjacent areas downstream.

The model extension centers on the addition of pollutant buildup, wash-off, transport and settling processes. The pollutants in runoff are varied. Typically, monitoring focuses on a select group of representative pollutants to provide timely and cost-effective assessment [63–65]. The use of surrogate pollutants as proxies for others is supported by research on the positive relationships between single pollutants and larger classes of pollutants [26,63,64,66–69]. Three of the more common pollutants to measure are total suspended solids (TSS), total nitrogen (TN), and total phosphorus (TP) [25,63,67]. TSS damages ecosystems by blocking light, engulfing plants, clogging stormwater infrastructure, and conveying other harmful pollutants like heavy metals and phosphorous [25]. Nutrient imbalances caused by nitrogen wreak havoc on ecosystems by changing the kinds of life that the water can support, for example, causing algae blooms or hypoxic conditions incapable of supporting animals [25,63,70]. Stormwater conveys washed-off pollutants, either as larger particulates (e.g., TSS, various metals), or dissolved (e.g., nitrogen and phosphorous compounds, various other dissolved solids) [66]. TSS are the most common solids, while nitrogen is more commonly present as dissolved [64,71]. Thus, TSS and TN are reasonable surrogates for other pollutants, and are the ones represented in L-GrID-WQ.

2.2.2.1. Initialization: pollutant buildup. Initialization of the model includes depositing buildup. The model assumes daily rates for a linear pollutant buildup derived from annual accumulation for each land cover. The user can customize these totals for local conditions. A slider sets the number of days of pollutant buildup on cell surfaces, which for this study is 10 days. The initial buildup for each land cover is the product of the corresponding daily rate and the number of accumulation days (see Appendix).

2.2.2.2. Pollutant wash-off. The force of the precipitation causes solids to erode and become suspended in the runoff (as with TSS) or to dissolve (TN). The equation for wash-off (Equation (1)) follows [72] and [73], who developed the most commonly used approach [48]:

$$w_{p,t} = k_w \times {q_t}^{n_w} \times m_{B,p,t} \quad (1)$$

Where.

$w_{p,t}$ = wash-off of pollutant p at time t
k_w = a pollutant wash-off coefficient
q_t = the rainfall rate in mm/time step at time t
n_w = a wash-off exponent in mm/time step at time t
$m_{B,p,t}$ = the mass buildup of pollutant p at time t

Values for coefficients and exponents can be selected by the user and calibrated to yield reasonable wash-off amounts as recommended by Rossman [48] (see Section 2.3).

2.2.2.3. Pollutant transport. Surface water is assumed to be mixed with uniform pollutant concentrations. The procedure for pollutant

transport in L-GriD-WQ builds on the surface flow procedure for L-GrID. When water moves from one cell to a neighboring cell, the destination cell recalculates the pollutant concentration by averaging the prior concentration with that of the incoming water, weighted by the amount of water held in the destination cell and the amount of water transferred. TN and TSS can leave the neighborhood through sewers or when surface water flows out of the landscape through boundary surface connections (e.g., road outlets). TN can infiltrate into soils and TSS can settle once water velocity is below a user-defined threshold (see Section 2.3 for details on threshold selection). Evaporation increases concentrations of pollutants and, if all water evaporates, pollutants are deposited onto land surfaces.

2.2.2.4. TSS settling. Settling of TSS due to gravity will be triggered if the average velocity of incoming water from surface flows falls below a threshold set by the user. The approach taken by L-GrID-WQ for the amount of settling at each time step uses the equations developed by Kadlec & Knight [74] and adapted by Rossman [48] (see Section 2.3 for details on parameterization):

$$c_{t+1} = c^* + (c_t - c^*)\exp\left(-\frac{k\Delta t}{d}\right) \quad (5)$$

Where:

c = the concentration of TSS.
c^* = minimum concentration of water below which settling will not occur
$k\Delta t$ = a settling coefficient
d = the depth of water at time t.

2.3. Parameterization and sensitivity to model extensions

The parameterization for the pollution processes in L-GrID-WQ was derived initially from literature and refined through sensitivity testing. With a precipitation total for a five-year 24-h storm in Chicago of 109.22 mm (see Appendix), and 0.1096 kg of TSS initial buildup per road cell (see Section 2.2.2.1 for calculation), we systematically tested different combinations of the two wash-off coefficients, k_w and n_w using ranges that encompassed values from Refs. [47,48]. The combination of $k_w = 0.016$ and $n_w = 1.1$ yielded a cumulative 75% TSS wash-off, which is reasonable for this area (John Watson, MWRD, pers. comm., 2021). Wash-off per time step follows precipitation rates, as expected. The mechanism for TN wash-off is identical to TSS, so the wash-off percent is the same.

For TSS settling, parameters were derived from Rossman [48] for the velocity threshold for pollutant settling; c^*, minimum non-removable concentration of TSS, and $k\Delta t$, a settling coefficient. Similar to the parametrization above, we swept different combinations of the three settling parameters. A velocity threshold of 0.0017 km/min, $c^* = 0.0005$ kg/cubic meters, and $k\Delta t = 5000$ mm/min produced 10% of TSS settlement within two days, which is typical in those conditions (ibid).

We conducted tests for the wash-off and settling parameters with a landscape described in Section 2.3.1 and default parameter values (Appendix A). Results were slightly sensitive to changes in k_w, where the % wash-off change was less than the % change of k_w, but were more sensitive to n_w, where wash-off change was around ±6%, higher than the input parameter change of ±5%. Sensitivity to TSS settling parameters was also mixed: it was not sensitive to $k\Delta t$ (no change in TSS settling), lightly sensitive to the velocity threshold (variations in TSS settling were smaller than the % change of the input parameter), and sensitive to c^*, where TSS settling change was between −7.4 and + 7.8%, relative to the ±5% input variation. This affects other outputs of interest, such as sewer load—the greater the settling, the lower the load.

Finally, we tested the sensitivity of the model to time step duration. We assume that simulations should use the largest time step possible that produces continuous flow. All simulations using time steps of ≤1 min produced stable outcomes; time steps of ≥2 min produced discontinuous flows due to issues with numerical aggregation. Thus, we selected time steps of 1 min for the simulations below.

2.3.1. Evaluation of the flooding algorithm

The University of Illinois at Chicago (UIC) Office of Sustainability commissioned a study to explore how GI could alleviate campus flooding on the West Campus. The West Campus is centered around the Illinois Medical District (IMD) and includes a variety of medical buildings belonging to the University of Illinois and other public and private institutions. This area also has significant amounts of surface parking lots and is bounded by an interstate to the north and dense mixed-use inner-city neighborhoods on its other sides. The study area is 52.82 ha, of which 44.32 ha (84%) is impervious cover, greatly limiting—spatially and financially—the opportunities for GI interventions.

The study area is very flat, so flooding conditions are driven by small local variations in elevation (street and sidewalk grading) and infrastructure conditions (blockages and malfunctions). With its concentration of medical facilities, maintaining access to the area is essential, but conflicts between the large institutions and the City of Chicago about the ownership of streets has resulted in underperforming sewer infrastructure, poorly and improperly graded roads prone to persistent water ponding, and uneven sidewalks and curbs that do not effectively channel water away from buildings. UIC was planning extensive capital investments, which included new buildings on green spaces and parking lots and the reconfiguration of streets, walkways, and other public spaces. To inform this decision-making process, we first evaluated L-GrID's flooding algorithm and then used the model to test different GI scenarios with L-GrID-WQ.

Landscape input files were created from public datasets and an in-person survey of the area by the authors. Elevation data came

from the Illinois State Geological Survey [75]. Land cover, including streets, was created based on public datasets from the City of Chicago [76,77] and visual comparisons with aerial photos in Google Maps. Soil types and sewer performance parameters build on prior work [37]. Neither the City of Chicago nor MWRD had a dataset of sewer locations, so the authors conducted an in-person survey of the campuses in 2018. This survey also provided information about locations with especially poorly graded streets and sidewalks and inlets with blockages that differed from the default settings. The final land cover and sewer inputs are shown in Fig. 3.

For model evaluation, UIC staff provided information about flooding problem areas in the campus, using either complaints or staff observations (Nicholas Haas, UIC, pers. comm., 2018). These were supplemented with data derived from Chicago's non-emergency complaint line (311) recording general public complaints (Anupam Verma, City of Chicago, pers. comm., 2019) (Fig. 4).

With 2-year, 24-h storms default parameters, L-GrID-WQ recreated the overall flooding patterns identified in the neighborhood (Fig. 5). The problem areas line up with those simulated, producing the worst flooding along Polk, Taylor, Wolcott, and Wood. Some flooding in higher elevation areas (see Fig. 4) could not be reproduced, in particular those along Damen and Roosevelt. The precision of the DEM elevations (1 m) made it impossible to capture all micro-variations that exist in the field, and in a very flat landscape these variations matter. Nonetheless, the institutional managers confirmed that the simulation results were reasonable and explainable, even for the places where model results differed from the data. One example of such a discrepancy is a small, depressed stretch of pavement with no working sewer inlet (the two adjacent problem areas on Damen near Polk). While the flooded area was small, it had a big impact on pedestrians. Examining such discrepancies supported stakeholder insights about whether flooding solutions should focus on installing new GI or on fixing existing sewer infrastructure instead. The evaluation helped reveal the best options for GI solutions, explored below (Section 2.3.3).

2.3.2. L-GrID-WQ output metrics for green infrastructure planning

In addition to the built-in monetary and flooding outputs, a list of impact metrics were developed with the UIC staff to reflect their flooding concerns and explore the benefits of specific GI plans. For easy comparison across scenarios, results are provided, where applicable, relative to a baseline with no GI (i.e., the difference with the baseline or the percentage point change) (Table 1).

Water quantity metrics answer two types of questions: the destination of water, and how well the GI captured runoff. To track where water went, we use the proportion of precipitation that goes to sewers or leaves the landscape through overland flow to downstream areas, and the percent of the cells that have ever been flooded (>1" of ponded water) during a run. To measure GI performance and efficiency in more detail, the model reports the percent of GI capacity filled with water (soil and surface storage) as an indicator of underutilization or excess investment. Another metric of efficiency is the cost in dollars per gallon of runoff captured by GI, per storm. While there would be numerous storms over the lifecycle of a GI installation, the comparisons across scenarios can give a sense of relative improvement in terms of this metric.

Water quality metrics answer questions about pollutant load reduction. The model reports the percent of wash-off that: a) goes to sewers (TSS and TN) (sewer capture), b) left the landscape through surface flows (TSS and TN) (downstream runoff), c) infiltrated into GI soils (TN) (infiltration), d) settled due to low surface flow velocity (TSS) (settling), and e) remained suspended (TSS) or dissolved (TN) in residual ponded water or redeposited after ponded water dries up (redeposited). Redeposited wash-off will cause higher local levels of pollutants, which can become a problem in future storm events as they are recirculated. Because high values for this metric can momentarily relieve pollutant exports, but low values can reduce pollutant exports in the future, we do not discuss the desirability of either outcome; we thus limit our discussion to reporting it so wash-off metrics total 100%. Other kinds of GI benefits, such as heat mitigation or habitat provision, are beyond the scope of this study.

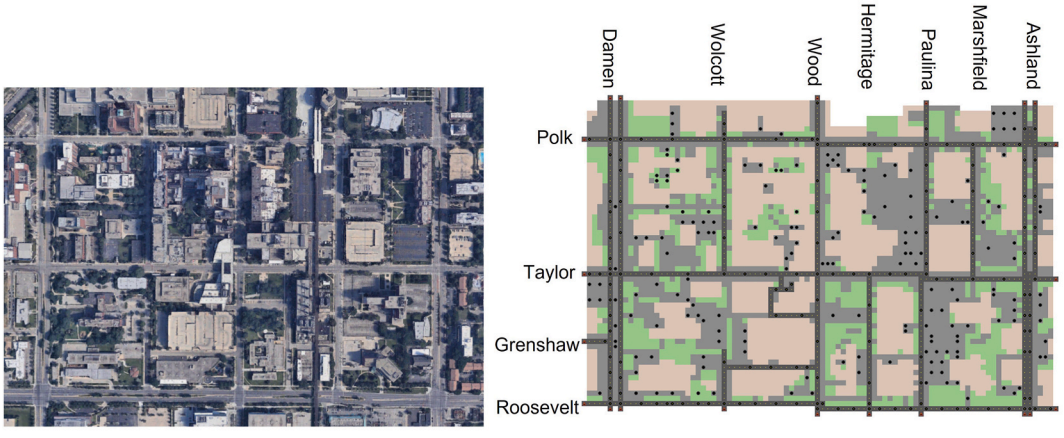

Fig. 3. Aerial photos of West Campus (left; Google, 2018) and L-GrID-WQ representation of the same area (right; brown = buildings; green = permeable surfaces, e.g., lawns; dark gray = roads; light gray = other impervious surfaces, e.g., walkways, sidewalks, and parking lots; black dots = locations of sewer inlets). (For interpretation of the references to colour in this figure legend, the reader is referred to the Web version of this article.)

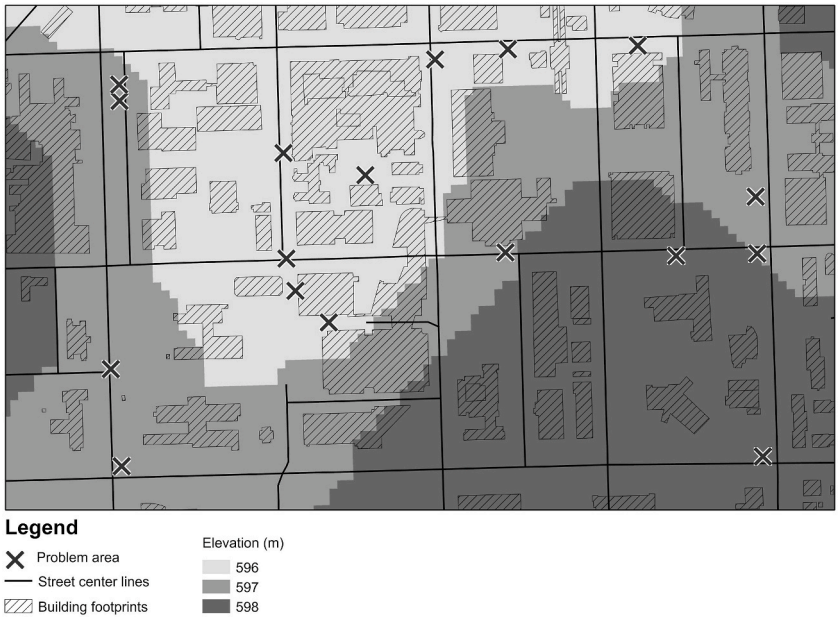

Fig. 4. Elevations of the west campus, university of Illinois at Chicago.

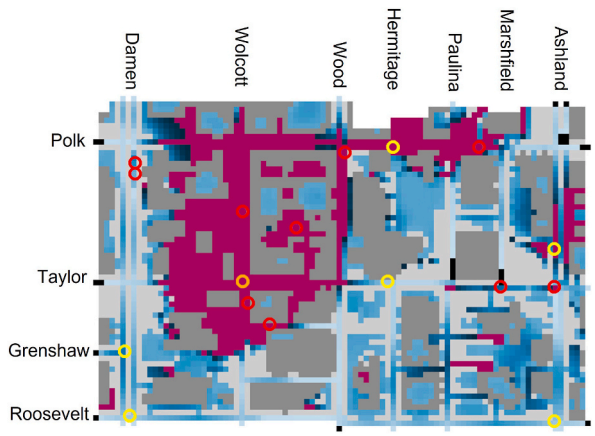

Fig. 5. Baseline flooding conditions. Magenta = water spilling over curbs or ponding above flooding threshold of 25.4 mm; blue = water ponding below flooding threshold (darker to lighter gradient shows decreasing water depth). Red circles = UIC flooding data; yellow circles = 311 flooding data; orange circles = overlapping UIC and 311 data. Gray = land cover (black = roads; dark gray = buildings; light gray = other). (For interpretation of the references to colour in this figure legend, the reader is referred to the Web version of this article.)

2.3.3. Green infrastructure scenarios

After establishing the baseline conditions for each storm type, we created with UIC staff a set of scenarios with different GI layouts. For a systematic review, we designed scenarios with the same spatial coverage of infrastructure (70 GI cells, a total of 0.7 ha), but different types and spatial distribution of GI. This GI coverage (1.3% of the landscape) was suggested by UIC, given the spatial and financial constraints of working in a dense urban neighborhood. The results of all scenarios are provided as a relative value, compared to the baseline conditions without GI; i.e., a negative value means that the output metric decreased with the application of GI, while a positive value means that the output metric increased in that GI scenario.

The baseline simulation results guided the GI location by identifying areas of water accumulation due to low elevations, proximity to roads, and poor drainage and grading (Fig. 6). These locations were primarily along Polk Street, Taylor Street, Wolcott Avenue, and Wood Street, and extending from these roads into neighborhood blocks. UIC staff also informed the scenario development with knowledge of budgetary and spatial constraints, as well as desirable GI types. Permeable pavers and bioswales were chosen due to their large storage volumes and infiltration capacity compared to rain barrels or green roofs (see Appendix).

The scenarios were developed to test the performance of permeable pavers and bioswales in two types of storms, chosen to reflect the sewer design conditions (2-year, 6-h) and a larger storm (5-year, 24-h) that is increasingly common due to climate change.

Table 1
Description of simulation metrics, relative to the baseline without GI where applicable.

Domain of variables	Metric	Description
All	Cost: install + maintain	Net present value ($) of installation of GI and 21 years of maintenance (initial year + 20 additional years)
Flooding	$ per gallon captured by GI	Dollars per gallon of water captured by GI
	GI capacity used	Percentage of GI capacity filled with water (soil and surface storage).
	Sewer capture	Percentage of precipitation captured by sewers
	Downstream runoff	Percentage of precipitation that left landscape through overland flow connections
	Area flooded	Percentage of cells that had at least 1 inch of ponded water at any point during the simulation
TN	% Wash-off	% of accumulated TN that washed off cells' surfaces
	Sewer capture	Percentage of TN wash-off captured by sewers
	Downstream runoff	Percentage of TN wash-off that left landscape through overland flow connections
	Infiltration	Percentage of TN wash-off that infiltrated
	Redeposited	Percentage of TN wash-off redeposited after ponded water dried or still dissolved in residual ponded water
TSS	% Wash-off	% of accumulated TSS that washed off cells' surfaces
	Sewer capture	Percentage of TSS wash-off captured by sewers
	Downstream runoff	Percentage of TSS wash-off that left landscape through overland flow connections
	Settling	Percentage of TSS wash-off that settled
	Redeposited	Percentage of TSS wash-off redeposited after ponded water dried or still suspended in residual ponded water

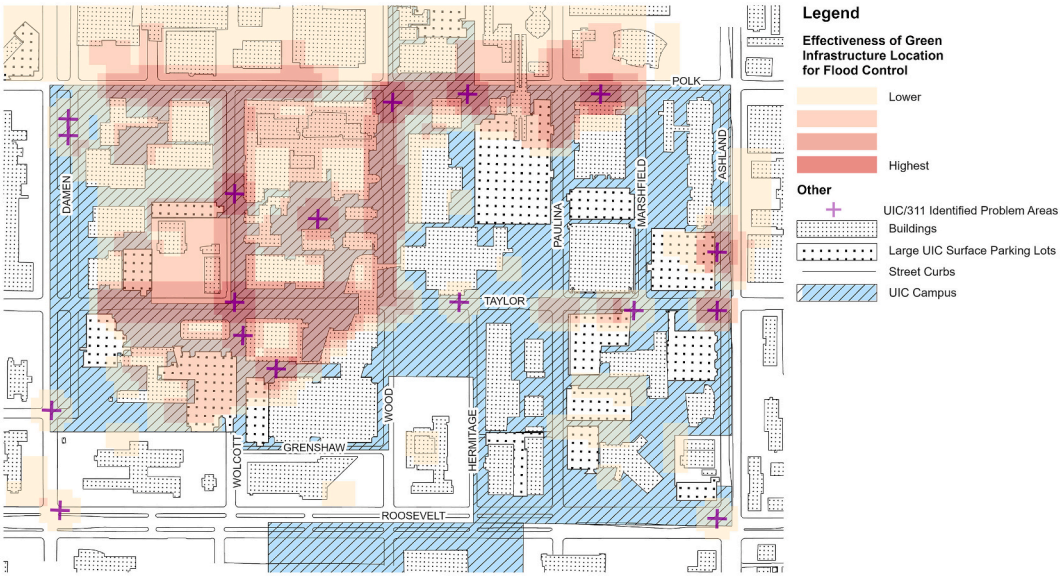

Fig. 6. Anticipated water accumulation areas based on the L-GrID-WQ baseline simulation and flooding data.

Although an assessment of a best case would assume dry initial conditions for soil and the sewer system, we assumed more realistic wet conditions at the start of a storm. Hydrological assumptions, including precipitation totals and other initial conditions, are listed in the Appendix. The impacts of each GI scenario were evaluated with the metrics in Table 1.

The installation and maintenance costs for all scenarios were on average $4 million, which is what UIC might have expected to spend in a larger-scale project. Scenarios with pavers had total costs of around $3.6 million and those with bioswales were around $4.4 million.

We designed five GI scenarios that used three different placement strategies: random (two layout scenarios: one with pavers and one with bioswales), curb-cuts (only bioswales located exclusively alongside curbs or roads), and flow-path (two layout scenarios: one with pavers and one with bioswales), which were the best performing scenarios in Zellner et al. [37]. Random layouts represent an opportunistic approach to GI installation as conditions on the ground and funding allow; for example, a lawn regrading might create an opportunity to install bioswales. The curb-cut layout only applies to bioswales because permeable pavers cannot be recessed to allow flows from roads. The flow-path layout is designed to intercept water where it is flowing and ponding across the landscape. This type of placement increases the contact of GI with stormwater. Fig. 6 guided the placement of curb-cut and flow-path placements. Layouts are shown in Fig. 7.

3. Simulation results

Simulation results of the scenarios outlined in the previous section are organized by effect of green infrastructure type and effect of

Fig. 7. GI scenarios, organized by GI type and placement strategy. Black = roads; dark gray = buildings; light gray = other land covers. Orange = permeable pavers; magenta = bioswales. (For interpretation of the references to colour in this figure legend, the reader is referred to the Web version of this article.)

spatial layout on flooding and on pollution. Where applicable, numerical results are shown as the change in outcomes compared to a baseline with no GI (i.e., the difference with the baseline or percentage point change) (Table 2 through Table 4).

3.1. Effect of green infrastructure type

Scenarios using only bioswales produced the best outcomes across all storm types (see Table 2 through Table 4). For most metrics the differences were small (within 8%), except for $ per gallon captured by GI and GI capacity used. The amount of runoff that reaches GI is a crucial factor in how much stormwater GI captures, which in turn is a function of the neighborhood-level design. Bioswales can be strategically located in more areas than permeable pavers, which are restricted to roads, alleyways, and driveways. While permeable pavers are very effective at the site level, substantial grading changes at a neighborhood level would be needed for pavers to infiltrate amounts similar to those captured by bioswales. The possibility of such re-grading is often limited in complex urban environments and would thus substantially increase the installation costs of pavers. While bioswale performance would also be improved by such grade changes, even without them, their surface depressions more readily collect runoff from their immediate surroundings. When bioswales are located next to roads, the curb-cuts make it even easier for water to reach them. Bioswale surface storage ensures

Table 2
Flooding output metrics for GI spatial layout scenarios for 2-year, 6-h and 5-year, 24-h storm simulations. See Section 2.3.2 or Table 1 for a complete definition of these metrics. Change relative to the baseline (without GI) is shown in parentheses. Precipitation not accounted for in sewer capture or downstream runoff has infiltrated the soil, remained as standing water, or evaporated.

2-year, 6-h storms						
	Cost: install + maintain	$ per gallon captured by GI	GI capacity used	% of precipitation		Area flooded
				Sewer capture	Downstream runoff	
No GI	$ -	$ -	0.0%	82.4%	8.7%	13.3%
Random - pavers	$ 3,638,670.00	$ 18.03	47.1%	81.7% (−0.7%)	7.5% (−1.2%)	12% (−1.3%)
Random - bioswales	$ 4,476,430.00	$ 6.27	79.4%	79.8% (−2.6%)	5.8% (−2.9%)	7.1% (−6.2%)
Curb-cuts - bioswales	$ 4,476,430.00	$ 5.42	91.8%	79.2% (−3.2%)	4.9% (−3.8%)	6.2% (−7.1%)
Flow-path - pavers	$ 3,638,670.00	$ 16.76	50.7%	81.7% (−0.7%)	7.7% (−1.1%)	11.5% (−1.8%)
Flow-path - bioswales	$ 4,476,430.00	$ 5.35	92.9%	78.9% (−3.5%)	5.3% (−3.4%)	5.8% (−7.4%)
5-year, 24-h storms						
	Cost: install + maintain	$ per gallon captured by GI	GI capacity used	% of precipitation		Area flooded
				Sewer capture	Downstream runoff	
No GI	$ -	$ -	0.0%	51.8%	23.7%	22.8%
Random - pavers	$ 3,638,670.00	$ 16.66	51.0%	51.8% (0%)	22.6% (−1%)	22.6% (−0.2%)
Random - bioswales	$ 4,476,430.00	$ 5.25	94.8%	51.8% (0%)	20.5% (−3.2%)	21.8% (−1%)
Curb-cuts - bioswales	$ 4,476,430.00	$ 5.16	96.4%	51.7% (0%)	20.2% (−3.5%)	21.7% (−1.1%)
Flow-path - pavers	$ 3,638,670.00	$ 16.54	51.4%	51.8% (0%)	22.6% (−1.1%)	22.4% (−0.4%)
Flow-path - bioswales	$ 4,476,430.00	$ 5.08	98.0%	51.8% (0%)	20.3% (−3.3%)	21.6% (−1.2%)

the retention of water even when high run-on rates surpass infiltration capabilities, which is not the case when run-on surpasses paver infiltration rates. These results suggest that permeable pavers should only be used when local circumstances make other GI types impractical, e.g., when high-use impervious land cover, such as alleys and walkways in between close buildings, cannot be converted to bioswales, or when more extensive landscape grading can direct water toward pavers and keep it there. For some metrics, pavers placed in a flow-path layout performed the same or slightly better than pavers placed randomly, but the differences are small. Thus, the remainder of our analysis focuses on the effectiveness of bioswale layouts.

3.2. Effects of green infrastructure layouts on flooding

In the baseline condition (without GI), 82.4% of stormwater was taken up by sewers in small storms, and 51.8% in large storms, as more flooding and runoff is produced relative to the limited sewer capacity. GI layouts made no impact on the proportion of sewer capture for larger storms; the system was overwhelmed by the amount of stormwater, and differences across spatial layouts were not substantial. This also aligns with prior studies [37,78–80].

Consistent with Zellner et al. [37], curb-cut layout and flow-path scenarios performed better than random placement in all dimensions and for the same reasons—the greater exposure of those layouts to water ponding along roads (Table 2). The flow-path layout performed best in all but one flooding metric. All three bioswale scenarios were similar in their monetary efficiency ($5.33 - $6.26 per gallon of water captured for 2-year storms and $5.07 - $5.24 for 5-year storms). In the curb-cut and flow-path layouts, GI capacity used approached 100% and area flooded was reduced by more than half. The three bioswale layouts reduced sewer capture by 2.6%–3.5% in smaller storms. While small, any local reduction in sewer loading reduces treatment costs and frees up sewer capacity elsewhere.

Downstream runoff decreased by 2.9%–3.4% in smaller storms. Here the effectiveness was flipped, where the curb-cut layout outperformed the flow-path layout. The curb-cut layout has greater amounts of GI located on the roads that leave the landscape, so it more effectively intercepts runoff flowing toward neighborhood outlets. Conversely, the flow-path layout has more GI located in the center of the landscape where water ponds and thus more effectively reduces area flooded and improves other metrics. For broader impact, both strategies can be combined to be tailored to a landscape by adapting the flow-path layout to place more bioswales along those roads that, like in the curb-cut layout, tend to channel more runoff towards outlets due to elevation.

3.3. Effects of green infrastructure layouts on pollution

In the baseline condition (without GI), 54.4% of accumulated TN and TSS washed off in small storms and 74.8% washed off in large

storms.

The curb-cut layout performed slightly better than the flow-path layout in most metrics (Table 3 and Table 4)—a reversal of the findings above. This suggests there may be tradeoffs between stormwater volume and quality management goals across layouts. Our flow-path layout was designed to prioritize flood control in low-lying areas (Fig. 6). The curb-cut layout, however, is closer to land covers with the highest pollutant generation rates (roads and impervious cover exclusive of buildings and other curbed paved areas). For example, every bioswale in the curb-cut layout borders at least three cells with the highest pollutant generation category. In contrast, some bioswales in the flow-path have no such neighbors. Bioswales farther from high pollutant generation will initially infiltrate relatively clean water while bioswales next to roads will immediately intercept dirtier water. Flow-path layout bioswales will eventually receive more polluted water but due to soil saturation, they will be unable to infiltrate it, leaving it on the surface. Curb-cut bioswales will also lower velocities of channelized water in streets, resulting in more TSS settling.

4. Discussion

We have evaluated the flooding algorithm in the L-GrID model, which was able to replicate reported flooding patterns, thus increasing the confidence with which it can be used to understand the causes of neighborhood flooding, identify problem areas to target with GI planning, and design and assess GI layouts to address this problem. We also extended L-GrID to account for stormwater quality through two proxies for water pollution, TSS and TN, and to represent a broader range of GI types. We applied this extended model, L-GrID-WQ, to a case in Chicago, Illinois, USA, and worked with stakeholders to examine the potential effectiveness of different GI scenarios to address stormwater management in their neighborhood in terms of both quantity and quality. The purpose of this study was to show how and why distinct GI strategies may be more or less advantageous, and tradeoffs across stormwater management functions may emerge from each one of these strategies.

Bioswales are the best performing type of GI, over all others, even as the differences between strategies were small for most—but not all—metrics in the scenarios tested here. This implies that their use should be prioritized whenever possible. The next best performing was permeable pavers, which may be a feasible alternative where spatial constraints limit the use of bioswales. Rain barrels alone do not contribute much to flooding control. While underground storage tanks may, retrofitting existing buildings with them may be too onerous. New construction, however, may create opportunities for this GI type, but its lack of flexibility to adapt to changing conditions should likely be considered relative to its cost. Finally, green roofs are both expensive and ineffective for flooding control, although other ecosystem services, like heat mitigation, may make them desirable.

Of the spatial layouts examined, both flow-path and curb-cuts performed the best, since they place GI where water can most easily reach them. These results confirm prior work [37,51,81,82] and can be promoted as an effective strategy to address neighborhood flooding. A critical insight from this study is that there may be spatial tradeoffs among different GI layouts, so that spatial allocations may provide benefits for different management goals. The concentration of bioswales should be prioritized in low-lying areas, whereas curb-cuts render the greatest benefits where runoff is faster (e.g., due to slope), where roads end in outlets from a neighborhood, and where pollution is a greater concern. GI layouts should thus be designed with attention to the heterogeneity in each landscape, to prioritize the most pressing concerns (water quantity or water quality) in different areas. While the differences explored here were relatively small, a more systematic study of these tradeoffs is warranted for an in-depth exploration of the effects of spatial GI layouts, combination of GI types, and percentage GI cover, individually and together. Such exploration would also help generalize these implications across a range of landscape and storm types.

An immediate priority for future work is to empirically validate the pollution component of L-GrID-WQ, as well as expand the

Table 3
TN-related metrics for GI spatial layout scenarios in for 2-year, 6-h and 5-year, 24-h storm simulations. See Section 2.3.2 or Table 1 for a complete definition of these metrics. Change relative to the baseline (without GI) is shown in parentheses.

2-year, 6-h storms					
	% Wash-off	% of wash-off			
		Sewer capture	Downstream runoff	Infiltration	Redeposited
No GI	58.4%	89.1%	8.2%	2.3%	0.4%
Random - pavers		87.6% (−1.5%)	7.1% (−1%)	4.9% (2.5%)	0.4% (0%)
Random - bioswales		87.3% (−1.8%)	5.9% (−2.2%)	5.1% (2.8%)	1.7% (1.3%)
Curb-cuts - bioswales		82.9% (−6.2%)	5.1% (−3.1%)	9.2% (6.8%)	2.9% (2.5%)
Flow-path - pavers		87.7% (−1.4%)	7.3% (−0.9%)	4.6% (2.2%)	0.4% (0%)
Flow-path - bioswales		83.2% (−5.9%)	5.4% (−2.8%)	8.5% (6.1%)	2.9% (2.5%)
5-year, 24-h storms					
	% Wash-off	% of wash-off			
		Sewer capture	Downstream runoff	Infiltration	Redeposited
No GI	74.8%	69.4%	20.2%	4.8%	5.6%
Random - pavers		68.6% (−0.8%)	19.2% (−1.1%)	7% (2.2%)	5.3% (−0.3%)
Random - bioswales		69.1% (−0.3%)	17.7% (−2.5%)	7.3% (2.5%)	5.9% (0.2%)
Curb-cuts - bioswales		66.1% (−3.3%)	17.9% (−2.3%)	10.4% (5.6%)	5.7% (0%)
Flow-path - pavers		68.7% (−0.7%)	19.2% (−1%)	6.7% (1.9%)	5.4% (−0.3%)
Flow-path - bioswales		66.5% (−2.9%)	18% (−2.3%)	9.7% (4.9%)	5.9% (0.2%)

Table 4
TSS output metrics for GI spatial layout scenarios in for 2-year, 6-h and 5-year, 24-h storm simulations. See Section 2.3.2 or Table 1 for a complete definition of these metrics. Change relative to the baseline (without GI) is shown in parentheses.

2-year, 6-h storms					
	% Wash-off	% of wash-off			
		Sewer capture	Downstream runoff	Settling	Redeposited
No GI	58.4%	76.7%	6.7%	16.5%	0.1%
Random - pavers		76.1% (−0.6%)	5.8% (−0.9%)	17.9% (1.4%)	0.2% (0.1%)
Random - bioswales		75.3% (−1.4%)	4.7% (−2%)	18.3% (1.8%)	1.7% (1.6%)
Curb-cuts - bioswales		73.1% (−3.6%)	4% (−2.7%)	20.4% (3.9%)	2.5% (2.4%)
Flow-path - pavers		76.5% (−0.2%)	6% (−0.8%)	17.4% (0.9%)	0.2% (0.1%)
Flow-path - bioswales		73.3% (−3.4%)	4.4% (−2.4%)	19.7% (3.3%)	2.5% (2.5%)
5-year, 24-h storms					
	% Wash-off	% of wash-off			
		Sewer capture	Downstream runoff	Settling	Redeposited
No GI	74.8%	57.3%	18.6%	15.1%	9.1%
Random - pavers		57.1% (−0.2%)	17.6% (−1%)	16.6% (1.5%)	8.8% (−0.4%)
Random - bioswales		57.5% (0.2%)	16% (−2.5%)	17.2% (2.1%)	9.3% (0.2%)
Curb-cuts - bioswales		56.6% (−0.7%)	15.7% (−2.9%)	18.4% (3.3%)	9.4% (0.2%)
Flow-path - pavers		57.2% (−0.1%)	17.6% (−1%)	16.4% (1.3%)	8.8% (−0.3%)
Flow-path - bioswales		56.8% (−0.5%)	15.7% (−2.9%)	18.2% (3.2%)	9.3% (0.2%)

validation of flooding quantity beyond observational data. Such data is often hard to come by, as it is costly to measure. The growing use of sensor technology and of video-recorded data provide promising opportunities to create the datasets that would allow this form of validation in the near future. In the meantime, model docking—i.e. aligning models of different kinds to see how their results converge or diverge—can help determine how well L-GrID-WQ can replicate the behavior of more established hydrological and water pollution models, increasing the confidence in L-GrID-WQ as a planning tool for rapid GI scenario exploration and assessment. Additionally, by identifying areas of concern for flooding and pollution, the model can inform the design of data collection efforts to support more data-intensive modeling and monitoring needs.

An extension of L-GrID is underway to include other ecosystem functions of GI, like heat mitigation and effects on energy use, to increase the range of GI co-benefits that the model can explore. Green roofs, while not a key element to combat flooding, is likely an important strategy to address heat. Properly accounting for heat-related effects of GI and how they play out in space may yet again change the deliberation around the tradeoffs among scenarios that best support the various GI co-benefits.

Beyond the modeling studies and scholarly implications of our work, there are important practical implications of developing and using simple and adaptable models to support deliberation and decision-making with stakeholders. In addition to customization of inputs, the model's relative simplicity and transparency, together with the ability to collaboratively construct outputs, make L-GrID and L-GrID-WQ well-suited to help stakeholders understand results across dimensions, prioritize goals and target areas for intervention, and to design the combination of infrastructure installation and maintenance for that intervention. Models designed for scientific research or engineering do not usually lend themselves to use by non-experts, making the L-GrID suite a powerful toolkit to learn and plan in a range of decision-making settings. The novelty of our approach is in the model parsimony that allows for rapid and flexible scenario exploration and testing, while retaining the ability to replicate observed flooding. This ability enhances the confidence in the GI design insights derived from the use of these parsimonious tools, particularly in the absence of costly empirical data and modeling.

Credit authorship contribution statement

Moira L. Zellner: Writing – review & editing, Writing – original draft, Supervision, Software, Project administration, Methodology, Investigation, Funding acquisition, Formal analysis, Conceptualization. **Dean Massey:** Writing – review & editing, Visualization, Software, Formal analysis.

Declaration of competing interest

The authors declare the following financial interests/personal relationships which may be considered as potential competing interests: Moira Zellner reports funding was provided by University of Illinois Chicago, Office of Sustainability, which commissioned part of the study. Moira Zellner reports funding was provided by Northeastern University, College of Social Sciences and Humanities and the School of Public Policy and Urban Affairs, to expand on and complete this study. If there are other authors, they declare that they have no known competing financial interests or personal relationships that could have appeared to influence the work reported in this paper.

Appendix A

Table A.1
Landscape and process parameters. Also consult Zellner et al. [37] for more detail.

Pollutant buildup	Roads	Impervious	Other curbed paved	Building	Permeable
TN kg/ha/year [83]	8	8	3.9	3.9	0
TSS kg/ha/year [83]	400	400	250	250	3
Days	10				
Sewers					
Manhole volume (cubic meters)	2.18 *(John Watson, MWRD, pers. comm 2014)*				
Manhole sump	25% of manhole volume *(John Watson, MWRD, pers. comm 2014)*				
Sewer intake rate (no blockage) (cubic meters/min)	2.04 *(John Watson, MWRD, pers. comm 2014)*				
Default blockage	50% *(John Watson, MWRD, pers. comm 2014)*				
Stormwater treatment rate (cubic meters/min per cell)	0.000468 [84]				
GI monetary costs (see Section 2.2.1.2 for more detail)	**Permeable paver**	**Bioswale**	**Green roof**	**Rain barrel**	
Placeable on cell types	Impervious, alley	Impervious, permeable	Building	Building	
Installation ($ net present value; per 10 m × 10 m cell)	20,287 [85]	17,914 [85]	34,823 [86]	123 [85]	
Maintenance ($ net present value; installation year + 20 additional years; per 10 m × 10 m cell)	31,694 [85]	46,035 [85]	7240 [86]	0 [85]	
Installation + maintenance ($ net present value; per 10 m × 10 m cell)	51,982 [85]	63,949 [85]	42,063 [86]	123 [85]	
GI storage volumes (see Section 2.2.1.2 for more detail)	**Permeable paver**	**Bioswale**	**Green roof**	**Rain barrel**	
Surface storage (cubic meters per 10 m × 10 m cell)	–	20	–	–	
Soil storage (cubic meters per 10 m × 10 m cell)	–	36.667	–	–	
Extra (non-ground) storage (cubic meters per 10 m × 10 m cell)	–	–	2.54 [58]	0.227 [58]	
Total storage (cubic meters per 10 m × 10 m cell)	23.165	56.667	2.54	0.227	
Water Quality: wash-off and settling (see Section 2.3 for selection)					
Velocity threshold for TSS settling (km/min)	0.0017				
kΔt; a fitting parameter (mm/min)	5000				
C*; minimum concentration (kg/cubic meters)	0.0005				
Kw; a pollutant wash-off coefficient	0.016				
Nw; a wash-off exponent in mm/min	1.1				
Hydrological scenarios					
Storm scenario	2-year, 6-h storms		5-year, 24-h storms		
Storm scenarios and precipitation totals (mm) [87]	63.754		109.22		
Initial soil saturation, including green infrastructure	50%				
Initial sewer capacity (remaining capacity)	70%				
Soil, infiltration, and surface flow	**All impervious covers**	**Permeable cover**	**Permeable paver**	**Bioswale**	
Underlying soil	silty clay loam [88]				
Engineered soil	sandy clay loam [89]				
Maximum wetting depth (mm)	–	1219 [90]	609.6 [91]	914.4 [88]	
Surface storage (mm)	–	–	–	200 [25,92]	
Capillary suction (mm)	–	273 [92]	90 [91]	61.3 [92]	
Effective porosity	–	0.437 [92]	0.380 [91]	0.401 [92]	
Saturated hydraulic conductivity (mm/min)	–	0.033 [92]	0.6 [93]	1 [92]	
Roughness coefficient	0.0175 [94]	0.15 [45]	0.0175 [94]	0.24 [83]	
Paver underdrain depth (mm)	–	–	304.8 [91]	–	
Paver drain rate to sewers (cubic meters/min)	–	–	0.21 [91]	–	
Elevation and roads					
Elevation	30 m DEM [75] interpolated to 10 m				
Road curb height (mm)	127 [95]				
Other curb height (mm)	53.5 [95]				
Evaporation and evapotranspiration					
Evaporation (mm/day per)	3.5625 [96]				
Evapotranspiration (mm/day)	1.66 [97,98]				

References

[1] V. Masson-Delmotte, P. Zhai, A. Pirani, S.L. Connors, C. Péan, S. Berger, N. Caud, Y. Chen, L. Goldfarb, M.I. Gomis, Climate change 2021: the physical science basis, Contrib. Work. Group Sixth Assess. Rep. Intergov. Panel Clim. Change 2 (2021).

[2] K. Byun, C. Chiu, A.F. Hamlet, Effects of 21st century climate change on seasonal flow regimes and hydrologic extremes over the Midwest and Great Lakes region of the US, Sci. Total Environ. 650 (Part 1) (2019) 1261–1277, https://doi.org/10.1016/j.scitotenv.2018.09.063.

[3] K. Hayhoe, J. VanDorn, T. Croley II, N. Schlegal, D. Wuebbles, Regional climate change projections for Chicago and the US Great Lakes, J. Gt. Lakes Res. 36 (Supplement 2) (2010) 7–21, https://doi.org/10.1016/j.jglr.2010.03.012.

[4] A. Semadeni-Davies, C. Hernebring, G. Svensson, L.-G. Gustafsson, The impacts of climate change and urbanisation on drainage in Helsingborg, Sweden: combined sewer system, J. Hydrol. 350 (2008) 100–113, https://doi.org/10.1016/j.jhydrol.2007.05.028.

[5] P.A. Wilderer, Applying sustainable water management concepts in rural and urban areas: some thoughts about reasons, means and needs, Water Sci. Technol. 49 (2004) 7–16, https://doi.org/10.2166/wst.2004.0403.

[6] Q. Zhou, A review of sustainable urban drainage systems considering the climate change and urbanization impacts, Water 6 (2014) 976–992, https://doi.org/10.3390/w6040976.

[7] M. Muller, Adapting to climate change: water management for urban resilience, Environ. Urbanization 19 (2007) 99–113, https://doi.org/10.1177/0956247807076726.

[8] R. Coffey, M.J. Paul, J. Stamp, A. Hamilton, T. Johnson, A review of water quality responses to air temperature and precipitation changes 2: nutrients, algal blooms, sediment, pathogens, JAWRA J. Am. Water Resour. Assoc. 55 (2019) 844–868, https://doi.org/10.1111/1752-1688.12711.

[9] C.O. Wilson, Q. Weng, Simulating the impacts of future land use and climate changes on surface water quality in the Des Plaines River watershed, Chicago Metropolitan Statistical Area, Illinois, Sci. Total Environ. 409 (2011) 4387–4405, https://doi.org/10.1016/j.scitotenv.2011.07.001.

[10] M. Wang, D. Zhang, A. Adhityan, W.J. Ng, J. Dong, S.K. Tan, Assessing cost-effectiveness of bioretention on stormwater in response to climate change and urbanization for future scenarios, J. Hydrol. 543 (2016) 423–432, https://doi.org/10.1016/j.jhydrol.2016.10.019.

[11] A.K. Sharma, L. Vezzaro, H. Birch, K. Arnbjerg-Nielsen, P.S. Mikkelsen, Effect of climate change on stormwater runoff characteristics and treatment efficiencies of stormwater retention ponds: a case study from Denmark using TSS and Cu as indicator pollutants, SpringerPlus 5 (2016) 1984, https://doi.org/10.1186/s40064-016-3103-7.

[12] Q. Zhou, G. Leng, J. Su, Y. Ren, Comparison of urbanization and climate change impacts on urban flood volumes: importance of urban planning and drainage adaptation, Sci. Total Environ. 658 (2019) 24–33, https://doi.org/10.1016/j.scitotenv.2018.12.184.

[13] F. Babovic, A. Mijic, Economic evaluation of adaptation pathways for an urban drainage system experiencing deep uncertainty, Water 11 (2019) 531, https://doi.org/10.3390/w11030531.

[14] H. Arisz, B.C. Burrell, Urban drainage infrastructure planning and design considering climate change, in: 2006 IEEE EIC Clim. Change Conf., IEEE, 2006, pp. 1–9.

[15] P. Krebs, T.A. Larsen, Guiding the development of urban drainage systems by sustainability criteria, Water Sci. Technol. 35 (1997) 89–98, https://doi.org/10.1016/S0273-1223(97)00187-X.

[16] I.M. Voskamp, F.H.M. Van de Ven, Planning support system for climate adaptation: composing effective sets of blue-green measures to reduce urban vulnerability to extreme weather events, Build. Environ. 83 (2015) 159–167, https://doi.org/10.1016/j.buildenv.2014.07.018.

[17] I.M. Kourtis, V.A. Tsihrintzis, E.A. Baltas, Modelling of a Combined Sewer System and Evaluation of Mitigation Measures Using SWMM, Eur. Water, 2017, pp. 123–128.

[18] E. Eriksson, A. Baun, L. Scholes, A. Ledin, S. Ahlman, M. Revitt, C. Noutsopoulos, P.S. Mikkelsen, Selected stormwater priority pollutants — a European perspective, Sci. Total Environ. 383 (2007) 41–51, https://doi.org/10.1016/j.scitotenv.2007.05.028.

[19] J. Margot, L. Rossi, D.A. Barry, C. Holliger, A review of the fate of micropollutants in wastewater treatment plants, WIREs Water 2 (2015) 457–487, https://doi.org/10.1002/wat2.1090.

[20] H. Fowdar, T.H. Neo, S.L. Ong, J. Hu, D.T. McCarthy, Performance analysis of a stormwater green infrastructure model for flow and water quality predictions, J. Environ. Manag. 316 (2022) 115259, https://doi.org/10.1016/j.jenvman.2022.115259.

[21] M. Jaffe, M. Zellner, E. Minor, M. Gonzalez-Meler, L.B. Cotner, D. Massey, H. Ahmed, M. Elberts, H. Sprague, S. Wise, The Illinois Green Infrastructure Study. A Report to the Illinois Environmental Protection Agency on Criteria in Section 15 of Public Act 96-0026, the Illinois Green Infrastructure for Clean Water Act of 2009, Chicago, IL, 2010.

[22] C. Mei, J. Liu, H. Wang, Z. Yang, X. Ding, W. Shao, Integrated Assessments of Green Infrastructure for Flood Mitigation to Support Robust Decision-Making for Sponge City Construction in an Urbanized Watershed, AGU Fall Meet. Abstr., 2018, pp. NH43D–1073B, https://doi.org/10.1016/j.scitotenv.2018.05.199.

[23] J.J. Houle, R.M. Roseen, T.P. Ballestero, T.A. Puls, J. Sherrard, Comparison of maintenance cost, labor demands, and system performance for LID and conventional stormwater management, J. Environ. Eng. 139 (2013) 932–938, https://doi.org/10.1061/(ASCE)EE.1943-7870.0000698.

[24] K. Eckart, Z. McPhee, T. Bolisetti, Performance and implementation of low impact development–a review, Sci. Total Environ. 607 (608) (2017) 413–432, https://doi.org/10.1016/j.scitotenv.2017.06.254.

[25] M.A. Gonzalez-Meler, L. Cotner, D.A. Massey, M.L. Zellner, E.S. Minor, The environmental and ecological benefits of green infrastructure for stormwater runoff in urban areas, JSM Environ. Sci. Ecol. 1 (2) (2013) 1007.

[26] G.H. LeFevre, K.H. Paus, P. Natarajan, J.S. Gulliver, P.J. Novak, R.M. Hozalski, Review of dissolved pollutants in urban storm water and their removal and fate in bioretention cells, J. Environ. Eng. 141 (2015) 04014050, https://doi.org/10.1061/(ASCE)EE.1943-7870.0000876.

[27] C. Li, C. Peng, P.-C. Chiang, Y. Cai, X. Wang, Z. Yang, Mechanisms and applications of green infrastructure practices for stormwater control: a review, J. Hydrol. 568 (2019) 626–637, https://doi.org/10.1016/j.jhydrol.2018.10.074.

[28] L. Li, A.P. Davis, Urban stormwater runoff nitrogen composition and fate in bioretention systems, Environ. Sci. Technol. 48 (2014) 3403–3410. https://doi-org.ezproxy.neu.edu/10.1021/es4055302.

[29] C. Pyke, M.P. Warren, T. Johnson, J. LaGro, J. Scharfenberg, P. Groth, R. Freed, W. Schroeer, E. Main, Assessment of low impact development for managing stormwater with changing precipitation due to climate change, Landsc. Urban Plann. 103 (2011) 166–173, https://doi.org/10.1016/j.landurbplan.2011.07.006.

[30] D. Gallet, The Value of Green Infrastructure: a Guide to Recognizing its Economic, Environmental and Social Benefits, Water Environment Federation, 2011, pp. 924–928, in: https://www.accesswater.org/publications/proceedings/-298629/the-value-of-green-infrastructure–a-guide-to-recognizing-its-economic–environmental-and-social-benefits. (Accessed 6 November 2022).

[31] S.T. Lovell, J.R. Taylor, Supplying urban ecosystem services through multifunctional green infrastructure in the United States, Landsc, Ecol. 28 (2013) 1447–1463. https://doi-org.ezproxy.neu.edu/10.1007/s10980.

[32] S. Meerow, J.P. Newell, Urban resilience for whom, what, when, where, and why? Urban Geogr. 40 (2019) 309–329. https://doi-org.ezproxy.neu.edu/10.1080/02723638.2016.1206395.

[33] K. Zhang, T.F.M. Chui, Linking hydrological and bioecological benefits of green infrastructures across spatial scales–A literature review, Sci. Total Environ. 646 (2019) 1219–1231, https://doi.org/10.1016/j.scitotenv.2018.07.355.

[34] A. Alves, B. Gersonius, Z. Kapelan, Z. Vojinovic, A. Sanchez, Assessing the Co-Benefits of green-blue-grey infrastructure for sustainable urban flood risk management, J. Environ. Manag. 239 (2019) 244–254, https://doi.org/10.1016/j.jenvman.2019.03.036.

[35] C. Choi, P. Berry, A. Smith, The climate benefits, co-benefits, and trade-offs of green infrastructure: a systematic literature review, J. Environ. Manag. 291 (2021) 112583, https://doi.org/10.1016/j.jenvman.2021.112583.

[36] T.L. Moore, J.S. Gulliver, L. Stack, M.H. Simpson, Stormwater management and climate change: vulnerability and capacity for adaptation in urban and suburban contexts, Clim. Change 138 (2016) 491–504, https://doi.org/10.1007/s10584-016-1766-2.

[37] M. Zellner, D. Massey, E. Minor, M. Gonzalez-Meler, Exploring the effects of green infrastructure placement on neighborhood-level flooding via spatially explicit simulations, Comput. Environ. Urban Syst. 59 (2016) 116–128, https://doi.org/10.1016/j.compenvurbsys.2016.04.008.

[38] K. Pochwat, D. Słyś, S. Kordana, The temporal variability of a rainfall synthetic hyetograph for the dimensioning of stormwater retention tanks in small urban catchments, J. Hydrol. 549 (2017) 501–511, https://doi.org/10.1016/j.jhydrol.2017.04.026.

[39] O. Fryd, T. Dam, M.B. Jensen, A planning framework for sustainable urban drainage systems, Water Pol. 14 (2012) 865–886, https://doi.org/10.2166/wp.2012.025.
[40] L. Kapetas, R. Fenner, Integrating blue-green and grey infrastructure through an adaptation pathways approach to surface water flooding, Philos. Trans. R. Soc. A 378 (2020) 20190204, https://doi.org/10.1098/rsta.2019.0204.
[41] T.A. Larsen, W. Gujer, The concept of sustainable urban water management, Water Sci. Technol. 35 (1997) 3–10, https://doi.org/10.1016/S0273-1223(97)00179-0.
[42] D. Dagenais, I. Thomas, S. Paquette, Siting green stormwater infrastructure in a neighbourhood to maximise secondary benefits: lessons learned from a pilot project, Landsc. Res. 42 (2017) 195–210, https://doi.org/10.1080/01426397.2016.1228861.
[43] N. Le Floch, V. Pons, E.M. Hassan Abdalla, K. Alfredsen, Catchment scale effects of low impact development implementation scenarios at different urbanization densities, J. Hydrol. 612 (2022) 128178, https://doi.org/10.1016/j.jhydrol.2022.128178. Part B.
[44] L. Yang, J. Scheffran, H. Qin, Q. You, Climate-related flood risks and urban responses in the pearl river delta, China, reg, Environ. Change 15 (2015) 379–391, https://doi.org/10.1007/s10113-014-0651-7.
[45] United States Department of Agriculture, Urban Hydrology for Small Watersheds, Engineering Division, Soil Conservation Service, US Department of Agriculture, 1986.
[46] Y. Liu, L.M. Ahiablame, V.F. Bralts, B.A. Engel, Enhancing a rainfall-runoff model to assess the impacts of BMPs and LID practices on storm runoff, J. Environ. Manag. 147 (2015) 12–23, https://doi.org/10.1016/j.jenvman.2014.09.005.
[47] L. Shoemaker, J. Riverson, K. Alvi, J.X. Zhen, S. Paul, T. Rafi, SUSTAIN: A Framework for Placement of Best Management Practices in Urban Watersheds to Protect Water Quality, U.S. Environmental Protection Agency, Washington, DC, 2009.
[48] L.A. Rossman, Storm Water Management Model User's Manual Version 5.1, National Risk Management Research Laboratory, Office of Research and Development, U.S. Environmental Protection Agency, 2015.
[49] G. Davis, M. Sakpota, Musicx. https://wiki.ewater.org.au/display/MX1/MUSICX, 2022.
[50] DHI, MIKE URBAN Model Manager, MIKE Powered by DHI, Hørsholm, Denmark, N.D..
[51] T. Xu, B.A. Engel, X. Shi, L. Leng, H. Jia, S.L. Yu, Y. Liu, Marginal-cost-based greedy strategy (MCGS): fast and reliable optimization of low impact development (LID) layout, Sci. Total Environ. 640 (641) (2018) 570–580, https://doi.org/10.1016/j.scitotenv.2018.05.358.
[52] M. Zellner, G.A. García, F. Bert, D. Massey, M. Nosetto, Exploring reciprocal interactions between groundwater and land cover decisions in flat agricultural areas and variable climate, Environ. Model. Software 126 (2020) 104641.
[53] J. Chen, Y. Liu, M.W. Gitau, B.A. Engel, D.C. Flanagan, J.M. Harbor, Evaluation of the effectiveness of green infrastructure on hydrology and water quality in a combined sewer overflow community, Sci. Total Environ. 665 (2019) 69–79, https://doi.org/10.1016/j.scitotenv.2019.01.416.
[54] C.-F. Chen, M.-Y. Sheng, C.-L. Chang, S.-F. Kang, J.-Y. Lin, Application of the SUSTAIN Model to a watershed-scale case for water quality management, Water 6 (2014) 3575–3589, https://doi.org/10.3390/w6123575.
[55] F. Antolini, E. Tate, Location matters: a framework to investigate the spatial characteristics of distributed flood attenuation, Water 13 (2021) 2706, https://doi.org/10.3390/w13192706.
[56] S.L. Jiménez Ariza, J.A. Martínez, A.F. Muñoz, J.P. Quijano, J.P. Rodríguez, L.A. Camacho, M. Díaz-Granados, A multicriteria planning framework to locate and select sustainable urban drainage systems (SUDS) in consolidated urban areas, Sustainability 11 (2019) 2312, https://doi.org/10.3390/su11082312.
[57] U. Wilensky, NetLogo. http://ccl.northwestern.edu/netlogo/, 1999.
[58] Virginia Department of Environmental Quality, BMP design Specifications. https://www.deq.virginia.gov/water/stormwater/stormwater-construction/bmp-design-specifications, 2011.
[59] United States Bureau of Labor Statistics, CPI inflation calculator. https://www.bls.gov/data/inflation_calculator.htm, 2023.
[60] United States Environmental Protection Agency, National stormwater calculator mobile web-based app, Version 3.4.0, 2022. https://swcweb.epa.gov/stormwatercalculator/.
[61] Council of Economic Advisers, Discounting for Public Policy: Theory and Recent Evidence on the Merits of Updating the Discount Rate, Counc. Econ. Advis. Issue Brief, 2017.
[62] Board of Governors of the Federal Reserve System, March 22, 2023: FOMC Projections materials, accessible version. https://www.federalreserve.gov/monetarypolicy/fomcprojtabl20230322.htm, 2023. (Accessed 24 May 2023).
[63] S.E. Clark, C.Y. Siu, Effectiveness of TSS, TN, and TP as indicators of stormwater runoff pollutant concentration and partitioning, in: World Environ. Water Resour. Congr. 2011 Bear, Knowl. Sustain., 2011, pp. 691–699, https://doi.org/10.1061/41173(414)71.
[64] N.S. Miguntanna, P. Egodawatta, S. Kokot, A. Goonetilleke, Determination of a set of surrogate parameters to assess urban stormwater quality, Sci. Total Environ. 408 (2010) 6251–6259, https://doi.org/10.1016/j.scitotenv.2010.09.015.
[65] B. Shi, P. Wang, J. Jiang, R. Liu, Applying high-frequency surrogate measurements and a wavelet-ANN model to provide early warnings of rapid surface water quality anomalies, Sci. Total Environ. 610 (2018) 1390–1399, https://doi.org/10.1016/j.scitotenv.2017.08.232.
[66] M. Kayhanian, B.D. Fruchtman, J.S. Gulliver, C. Montanaro, E. Ranieri, S. Wuertz, Review of highway runoff characteristics: comparative analysis and universal implications, Water Res. 46 (2012) 6609–6624, https://doi.org/10.1016/j.watres.2012.07.026.
[67] A. Liu, P. Egodawatta, Y. Guan, A. Goonetilleke, Influence of rainfall and catchment characteristics on urban stormwater quality, Sci. Total Environ. 444 (2013) 255–262, https://doi.org/10.1016/j.scitotenv.2012.11.053.
[68] N.R. Thomson, E.A. McBean, W. Snodgrass, I.B. Monstrenko, Highway stormwater runoff quality: development of surrogate parameter relationships, Water Air Soil Pollut. 94 (1997) 307–347. https://doi-org.ezproxy.neu.edu/10.1007/BF02406066.
[69] B.G. Turner, M.C. Boner, Watershed monitoring and modelling and USA regulatory compliance, Water Sci. Technol. 50 (2004) 7–12, https://doi.org/10.2166/wst.2004.0666.
[70] S.R. Carpenter, N.F. Caraco, D.L. Correll, R.W. Howarth, A.N. Sharpley, V.H. Smith, Nonpoint pollution of surface waters with phosphorus and nitrogen, Ecol. Appl. 8 (1998) 559–568, https://doi.org/10.1890/1051-0761, 1998)008[0559:NPOSWW]2.0.CO;2.
[71] N.P. Miguntanna, A. Liu, P. Egodawatta, A. Goonetilleke, Characterising nutrients wash-off for effective urban stormwater treatment design, J. Environ. Manag. 120 (2013) 61–67, https://doi.org/10.1016/j.jenvman.2013.02.027.
[72] D.C. Ammon, Urban Stormwater Pollutant Buildup and Washoff Relationships, Master Thesis, University of Florida, 1979.
[73] J.D. Sartor, G.B. Boyd, Water Pollution Aspects of Street Surface Contaminants, Environmental Protection Agency, Washington, D.C, 1972.
[74] R.H. Kadlec, R.L. Knight, Treatment Wetlands, CRC Press, Boca Raton, Florida, 1996.
[75] Illinois State Geological Survey, Illinois statewide 30-meter digital elevation model. https://clearinghouse.isgs.illinois.edu/, 2003.
[76] City of Chicago, Street center lines. https://data.cityofchicago.org/browse?tags=gis, 2017. (Accessed 21 July 2017).
[77] City of Chicago, Building footprints. https://data.cityofchicago.org/browse?tags=gis, 2017. (Accessed 21 July 2017).
[78] L. Garcia-Cuerva, E.Z. Berglund, L. Rivers, An integrated approach to place Green Infrastructure strategies in marginalized communities and evaluate stormwater mitigation, J. Hydrol. 559 (2018) 648–660, https://doi.org/10.1016/j.jhydrol.2018.02.066.
[79] W. Liu, W. Chen, C. Peng, Assessing the effectiveness of green infrastructures on urban flooding reduction: a community scale study, Ecol. Model. 291 (2014) 6–14, https://doi.org/10.1016/j.ecolmodel.2014.07.012.
[80] S.H. Pour, A.K.A. Wahab, S. Shahid, M. Asaduzzaman, A. Dewan, Low impact development techniques to mitigate the impacts of climate-change-induced urban floods: current trends, issues and challenges, Sustain. Cities Soc. 62 (2020) 102373, https://doi.org/10.1016/j.scs.2020.102373.
[81] J.V. Loperfido, G.B. Noe, S.T. Jarnagin, D.M. Hogan, Effects of distributed and centralized stormwater best management practices and land cover on urban stream hydrology at the catchment scale, J. Hydrol. 519 (2014) 2584–2595, https://doi.org/10.1016/j.jhydrol.2014.07.007. Part C.
[82] W. Sohn, J. Bae, G. Newman, Green infrastructure for coastal flood protection: the longitudinal impacts of green infrastructure patterns on flood damage, Appl. Geogr. 135 (2021) 102565, https://doi.org/10.1016/j.apgeog.2021.102565.
[83] California department of transportation, biofiltration swale design guidance, 2009. (Accessed 3 December 2014).

[84] Metropolitan water reclamation District of greater Chicago, stickney water reclamation plant, 2014. (Accessed 18 November 2014).
[85] San Antonio River Authority, San Antonio River Basin Low Impact Development Technical Design Guidance Manual, v2, San Antonio, TX, 2019. https://www.sariverauthority.org/sites/default/files/2019-08/SARB%20LID%20Technical%20Design%20Manual%202nd%20Edition.pdf.
[86] Arup, San francisco living roof cost-benefit study. https://default.sfplanning.org/Citywide/livingroof/SFLivingRoofCost-BenefitStudyReport_060816.pdf, 2016.
[87] J. Angel, M. Markus, Frequency Distributions of Heavy Precipitation in Illinois: Updated Bulletin 70, ISWS Contract Rep. CR-2019-05, 2019.
[88] R. Krumm, D. Nelson, S. Beaverson, Master Data Set for Illinois, Soil Associations Map (500K), 1984.
[89] W.F. Hunt, W.G. Lord, Urban Waterways: Bioretention Performance, Design, Construction, and Maintenance, North Carolina State University, North Carolina Cooperative Extension Service, 2006. https://www.bae.ncsu.edu/extension/ext-publications/water/protecting/ag-588-05-bioretentionperformance-design-construction-maintenance.pdf.
[90] W.S. Morrow, J.B. Sharpe, Preliminary Assessment of the Potential for Inducing Stormwater Infiltration in Cook County, Illinois, US Department of the Interior, US Geological Survey, 2009.
[91] J. Zhang, Laboratory Scale Study of Infiltration from Pervious Pavements, PhD Thesis, RMIT University, 2006.
[92] B. Oram, Estimation of Green-Ampt Infiltration Parameters, (n.d.). http://www.water-research.net/Waterlibrary/Stormwater/greenamp.pdf (accessed October 27, 2010)..
[93] L. Chai, M. Kayhanian, B. Givens, J.T. Harvey, D. Jones, Hydraulic performance of fully permeable highway shoulder for storm water runoff management, J. Environ. Eng. 138 (2012) 711–722, https://doi.org/10.1061/(ASCE)EE.1943-7870.0000523.
[94] City of Dallas, Drainage design manual, 1993. http://www.dallascityhall.com/public_works/pdf/DrainageDesignManual-searchable.pdf.
[95] City of Chicago, Street and site plan design standards, 2007.
[96] (site 11-1497), Illinois State Climatologist Office, Monthly Pan Evaporation for Chicago Botanical Gardens, Glencoe, IL, 2008, http://www.isws.illinois.edu/atmos/statecli/Pan-Evap/panevapx.htm. (Accessed 30 November 2011).
[97] R.M. Lazzarin, F. Castellotti, F. Busato, Experimental measurements and numerical modelling of a green roof, Energy Build. 37 (2005) 1260–1267, https://doi.org/10.1016/j.enbuild.2005.02.001.
[98] H. Li, L.J. Sharkey, W.F. Hunt, A.P. Davis, Mitigation of impervious surface hydrology using bioretention in North Carolina and Maryland, J. Hydrol. Eng. 14 (2009) 407–415, 10.1061/ASCE)1084-0699(2009)14:4(407).